

Band-tunable color cone lasing emission based on dye-doped cholesteric liquid crystals with various pitches and a pitch gradient

C.-R. Lee,^{1,*} S.-H. Lin,¹ H.-C. Yeh,² and T.-D. Ji¹

¹*Institute of Electro-Optical Science and Engineering and Advanced Optoelectronic Technology Center, National Cheng Kung University, Tainan, Taiwan 701, Republic of China*
²*Graduate Institute of Electro-Optical Engineering, National Kaohsiung First University of Science and Technology, Kaohsiung, Taiwan 811, Republic of China*
**crlee@mail.ncku.edu.tw*

Abstract: This study elucidates, for the first time, a novel band-tunable color cone lasing emission (CCLE) based on dye-doped cholesteric liquid crystal (DDCLC) films with various pitches. For several CLC cells with different pitches it was shown experimentally that the lasing band on the CCLE can be tuned among various color regions measured within different angular ranges. Some important features of the tunable CCLE are also identified and discussed. A spatially band-tunable color cone laser, based on a single DDCLC with a gradient pitch, is developed as a real application.

©2009 Optical Society of America

OCIS codes: (230.3720) Liquid-crystal devices; (160.3710) Liquid crystals; (140.3600) Lasers, tunable; (140.3490) Lasers, distributed-feedback

References and links

1. J. P. Dowling, M. Scalora, M. J. Bloemer, and C. M. Bowden, "The photonic band edge laser: A new approach to gain enhancement," *J. Appl. Phys.* **75**(4), 1896–1899 (1994).
2. I. P. Il'chishin, E. A. Tikhonov, V. G. Tishchenko, and M. T. Shpak, "Generation of a tunable radiation by impurity cholesteric liquid crystals," *JETP Lett.* **32**, 24–27 (1980).
3. V. I. Kopp, B. Fan, H. K. M. Vithana, and A. Z. Genack, "Low-threshold lasing at the edge of a photonic stop band in cholesteric liquid crystals," *Opt. Lett.* **23**(21), 1707–1709 (1998).
4. V. I. Kopp, Z.-Q. Zhang, and A. Z. Genack, "Lasing in chiral photonic structures," *Prog. Quantum Electron.* **27**(6), 369–416 (2003).
5. H. Finkelmann, S. T. Kim, A. Muñoz, P. Palffy-Muhoray, and B. Taheri, "Tunable mirrorless lasing in cholesteric liquid crystalline elastomers," *Adv. Mater.* **13**(14), 1069–1072 (2001).
6. J. Schmidtke, W. Stille, H. Finkelmann, and S. T. Kim, "Laser emission in a dye doped cholesteric polymer network," *Adv. Mater.* **14**(10), 746–749 (2002).
7. T. Matsui, R. Ozaki, K. Funamoto, M. Ozaki, and K. Yoshino, "Flexible mirrorless laser based on a free-standing film of photopolymerized cholesteric liquid crystal," *Appl. Phys. Lett.* **81**(20), 3741–3743 (2002).
8. S. Furumi, S. Yokoyama, A. Otomo, and S. Mashiko, "Electrical control of the structure and lasing in chiral photonic band-gap liquid crystals," *Appl. Phys. Lett.* **82**(1), 16–18 (2003).
9. K. Bjorknas, E. P. Raynes, and S. Gilmour, "Effects of molecular shape on the photoluminescence of dyes embedded in a chiral polymer with a photonic band gap," *J. Mater. Sci. Mater. Electron.* **14**, 397–401 (2003).
10. J. Schmidtke, and W. Stille, "Fluorescence of a dye-doped cholesteric liquid crystal film in the region of the stop band: theory and experiment," *Eur. Phys. J. B* **31**(2), 179–194 (2003).
11. F. Araoka, K.-C. Shin, Y. Takanishi, K. Ishikawa, H. Takezoe, Z. Zhu, and T. M. Swager, "How doping a cholesteric liquid crystal with polymeric dye improves an order parameter and makes possible low threshold lasing," *J. Appl. Phys.* **94**(1), 279–283 (2003).
12. A. Chanishvili, G. Chilaya, G. Petriashvili, R. Barberi, R. Bartolino, G. Cipparrone, A. Mazzulla, and L. Oriol, "Phototunable lasing in dye-doped cholesteric liquid crystals," *Appl. Phys. Lett.* **83**(26), 5353–5355 (2003).
13. S. Furumi, S. Yokoyama, A. Otomo, and S. Mashiko, "Phototunable photonic bandgap in a chiral liquid crystal laser device," *Appl. Phys. Lett.* **84**(14), 2491–2493 (2004).
14. A. Fuh, T.-H. Lin, J.-H. Liu, and F.-C. Wu, "Lasing in chiral photonic liquid crystals and associated frequency tuning," *Opt. Express* **12**(9), 1857–1863 (2004).
15. S. G. Lukishova, A. W. Schmid, C. M. Supranowitz, N. Lippa, A. J. Mcnamara, R. W. Boyd, and C. R. Stroud, Jr., "Dye-doped cholesteric-liquid-crystal room-temperature single photon source," *J. Mod. Opt.* **51**(9-10) 1535–1547 (2004).
16. S. M. Morris, A. D. Ford, M. N. Pivnenko, and H. J. Coles, "Enhanced emission from liquid-crystal lasers," *J. Appl. Phys.* **97**, 023103 (2005).

17. A. Chanishvili, G. Chilaya, G. Petriashvili, R. Barberi, R. Bartolino, G. Cipparrone, A. Mazzulla, R. Gimenez, L. Oriol, and M. Pinol, "Widely tunable ultraviolet-visible liquid crystal laser," *Appl. Phys. Lett.* **86**(5), 051107 (2005).
18. P. V. Shibaev, R. L. Sanford, D. Chiappetta, V. Milner, A. Genack, and A. Bobrovsky, "Light controllable tuning and switching of lasing in chiral liquid crystals," *Opt. Express* **13**(7), 2358–2363 (2005).
19. T.-H. Lin, Y.-J. Chen, C.-H. Wu, and Y.-G. A. Fuh, J.-H. Liu, and P.-C. Yang, "Cholesteric liquid crystal laser with wide tuning capability," *Appl. Phys. Lett.* **86**(16), 161120 (2005).
20. H. Yu, B. Y. Tang, J. Li, and L. Li, "Electrically tunable lasers made from electro-optically active photonics band gap materials," *Opt. Express* **13**(18), 7243–7249 (2005).
21. Y. Zhou, Y. Huang, A. Rapaport, M. Bass, and S.-T. Wu, "Doubling the optical efficiency of a chiral liquid crystal laser using a reflector," *Appl. Phys. Lett.* **87**(23), 231107 (2005).
22. S. M. Morris, A. D. Ford, M. N. Pivnenko, and H. J. Coles, "The effects of reorientation on the emission properties of a photonic band edge liquid crystal laser," *J. Opt. A, Pure Appl. Opt.* **7**(5), 215–223 (2005).
23. M. H. Song, N. Y. Ha, K. Amemiya, B. Park, Y. Takanishi, K. Ishikawa, J. W. Wu, S. Nishimura, T. Toyooka, and H. Takezoe, "Defect-mode lasing with lowered threshold in a three-layered hetero-cholesteric liquid-crystal structure," *Adv. Mater.* **18**(2), 193–197 (2006).
24. Y. Huang, Y. Zhou, and S.-T. Wu, "Spatially tunable laser emission in dye-doped photonic liquid crystals," *Appl. Phys. Lett.* **88**(1), 011107 (2006).
25. Y. Zhou, Y. Huang, Z. Ge, L.-P. Chen, Q. Hong, T. X. Wu, and S. T. Wu, "Enhanced photonic band edge laser emission in a cholesteric liquid crystal resonator," *Phys. Rev. E Stat. Nonlin. Soft Matter Phys.* **74**(6), 061705 (2006).
26. S. M. Morris, A. D. Ford, M. N. Pivnenko, O. Haderler, and H. J. Coles, "Correlations between the performance characteristics of a liquid crystal laser and the macroscopic material properties," *Phys. Rev. E Stat. Nonlin. Soft Matter Phys.* **74**(6), 061709 (2006).
27. Y. Huang, Y. Zhou, C. Doyle, and S.-T. Wu, "Tuning the photonic band gap in cholesteric liquid crystals by temperature-dependent dopant solubility," *Opt. Express* **14**(3), 1236–1242 (2006).
28. Y. Matsuhisa, R. Ozaki, K. Yoshino, and M. Ozaki, "High Q defect mode and laser action in one-dimensional hybrid photonic crystal containing cholesteric liquid crystal," *Appl. Phys. Lett.* **89**(10), 101109 (2006).
29. G. Chilaya, A. Chanishvili, G. Petriashvili, R. Barberi, M. P. De Santo, and M. A. Matraga, "Enhancing cholesteric liquid crystal laser stability by cell rotation," *Opt. Express* **14**(21), 9939–9943 (2006).
30. Y. Zhou, Y. Huang, Z. Ge, L.-P. Chen, Q. Hong, T. X. Wu, and S.-T. Wu, "Enhanced photonic band edge laser emission in a cholesteric liquid crystal resonator," *Phys. Rev. E* **74**(6), 061705 (2006).
31. S. M. Jeong, K. Sonoyama, Y. Takanishi, K. Ishikawa, H. Takezoe, S. Nishimura, G. Suzuki, and M. H. Song, "Optical cavity with a double-layered cholesteric liquid crystal mirror and its prospective application to solid state laser," *Appl. Phys. Lett.* **89**(24), 241116 (2006).
32. Y. Matsuhisa, Y. Huang, Y. Zhou, S.-T. Wu, Y. Takao, A. Fujii, and M. Ozaki, "Cholesteric liquid crystal laser in a dielectric mirror cavity upon band-edge excitation," *Opt. Express* **15**(2), 616–622 (2007).
33. L. M. Blinov, G. Cipparrone, A. Mazzulla, P. Pagliusi, and V. V. Lazarev, "Lasing in cholesteric liquid crystal cells: Competition of Bragg and leaky modes," *J. Appl. Phys.* **101**(5), 053104 (2007).
34. Y. Matsuhisa, R. Ozaki, Y. Takao, and M. Ozaki, "Linearly polarized lasing in one-dimensional hybrid photonic crystal containing cholesteric liquid crystal," *J. Appl. Phys.* **101**(3), 033120 (2007).
35. Y. Matsuhisa, Y. Huang, Y. Zhou, S.-T. Wu, R. Ozaki, Y. Takao, A. Fujii, and M. Ozaki, "Low-threshold and high efficiency lasing upon band-edge excitation in a cholesteric liquid crystal," *Appl. Phys. Lett.* **90**(9), 091114 (2007).
36. Y. Zhou, E. E. Jang, Y. Huang, and S.-T. Wu, "Enhanced laser emission in opposite handedness using a cholesteric polymer film stack," *Opt. Express* **15**(6), 3470–3477 (2007).
37. K. Sonoyama, Y. Takanishi, K. Ishikawa, and H. Takezoe, "Position-sensitive cholesteric liquid crystal dye laser covering a full visible range," *Jpn. J. Appl. Phys.* **46**(36), L874–L876 (2007).
38. K. Dolgaleva, S. K. H. Wei, S. G. Lukishova, S. H. Chen, K. Schwert, and R. W. Boyd, "Enhanced laser performance of cholesteric liquid crystals doped with oligofluorene dye," *J. Opt. Soc. Am. B* **25**(9), 1496–1504 (2008).
39. M.-Y. Jeong, H. Choi, and J. W. Wu, "Spatial tuning of laser emission in a dye-doped cholesteric liquid crystal wedge cell," *Appl. Phys. Lett.* **92**(5), 051108 (2008).
40. C.-T. Wang, and T.-H. Lin, "Multi-wavelength laser emission in dye-doped photonic liquid crystals," *Opt. Exp.* **16**(22), 18334–18339 (2008).
41. B. Park, M. Kim, S. W. Kim, and I. T. Kim, "Circularly polarized unidirectional lasing from a cholesteric liquid crystal layer on a 1-D photonic crystal substrate," *Opt. Exp.* **17**(15), 12323–12331 (2009).
42. C.-R. Lee, S.-H. Lin, H.-C. Yeh, T.-D. Ji, K.-L. Lin, T.-S. Mo, C.-T. Kuo, K.-Y. Lo, S.-H. Chang, and Y.-G. Fuh, and S.-Y. Huang, "Color cone lasing emission in a dye-doped cholesteric liquid crystal with a single pitch," *Opt. Exp.* **17**(15), 12910–12921 (2009).
43. A. Sugita, H. Takezoe, Y. Ouchi, A. Fukuda, E. Kuze, and N. Goto, "Numerical calculation of optical eigenmodes in cholesteric liquid crystals by 4×4 matrix method," *Jpn. J. Appl. Phys.* **21**(Part 1, No. 11), 1543–1546 (1982).

1. Introduction

Planar cholesteric liquid crystals (CLCs) can be regarded as one-dimensional photonic crystals (1D PCs) with band gaps because of their spatially-periodic distribution of refractive index with a large modulation, in which rod-like LC molecules can rotate periodically along the so-called helical axis by interaction with the chiral dopants. Because of this gap feature, planar CLCs can be used as mirrorless distributed feedback resonators. By doping active dyes in the CLCs, the spontaneously emitted fluorescence will be suppressed within the gaps and instead enhanced at band edges. Principally, the multi-reflection of fluorescence at band edges can lead to a very small group velocity and very large density of photonic state (DOS) [1]. With the distributed feedback effect of the active multilayer of the resonator in the multi-reflection process, the rates of spontaneous and stimulated emissions for the fluorescence at band edges can both be amplified so that a high gain exceeding loss can be obtained to induce a low-threshold lasing emission [2–4].

In the last decade, lasers associated with dye-doped CLC (DDCLC) have been widely investigated because of the interesting fundamentals of their lasing mechanism and their wide range of potential applications [2–41]. Numerous studies have focused on thermally, optically, electrically and spatially-tunable features of such lasers based on external controllability of the CLC pitch [5,12–14,16–20,24,27,37,39]. The authors' recent report [42] demonstrated that a "single pitched" DDCLC laser can simultaneously emit a wide-band lasing emission with an angular dependence on the wavelength. This emission is called color cone lasing emission (CCLE). We observed for the first time for the CLC structure that significant part of lasing energy in Bragg modes is irradiated into wide angles. Angular dependence of dye fluorescence and lasing spectrum at the output of dye-doped CLC structure both for Bragg and leaky (waveguide) modes was studied earlier by Blinov *et al.* [33]. In Ref. 33 for Bragg modes angular dependence of wavelength was observed only for fluorescence but not for lasing in the angular range of 0° – 35° , although for leaky modes angular dependence of lasing wavelength was observed in the range 70° – 100° . The present work examines a band-tunable color cone laser in DDCLC cells using several cells with various pitches. The lasing band of the formed CCLE can be tuned among various color regions, measured within various ranges of oblique angle, as the CLC pitch is varied. Some unique lasing features of the tunable CCLE are identified and analyzed. As an example of a practical application, a spatially band-tunable color cone laser that is based on a single DDCLC cell with a pitch gradient is successfully developed.

2. Sample preparation and experimental setups

The nematic LC (NLC), left-handed chiral dopant and two kinds of laser dye used herein are ZLI2293 ($n_e = 1.6312$ and $n_o = 1.4990$ at 20°C) (from Merck), S811 (from Merck), and 4-Dicyanmethylene-2-methyl-6-(p-dimethylaminostyryl)-4H-pyran (DCM) and Pyrromethene 567 (P567) (from Exciton), respectively. Six different CLC mixtures, with different mixing ratios of ZLI2293:S811 with 73.52:26.48, 73.81:26.19, 74.82:25.18, 75.81:24.19, 76.82:23.18, and 77.71:22.29wt%, are prepared. The concentrations of DCM and P567 in each CLC mixture are 0.4 and 0.25wt%, respectively. Each empty cell is pre-fabricated with a same standard by combining two indium-tin-oxide-coated glass slides separated with two 25 μm -thick plastic spacers. Both glass slides in each empty cell are pre-coated with polyvinyl alcohol (PVA) film, and pre-rubbed in anti-parallel direction. The six dye-doped CLC mixtures above are then injected into six empty cells to form six different DDCLC cells, which are labeled as cells 1–6. These cells are then placed together in a clean and opaque specimen box at room temperature for about 10 days, so that the CLC in cells 1–6 has enough time to slowly self-organize into perfect planar structures with pitches $P_1 = 364.65$, $P_2 = 368.57$, $P_3 = 383.42$, $P_4 = 399.10$, $P_5 = 416.54\text{nm}$, and $P_6 = 433.04$, respectively.

This work utilizes two experimental setups for measuring the lasing and reflection spectra of the DDCLC cells at different oblique angles. The experimental setups and associated method for measurement can be found in the authors' previous work and are not repeated

herein [42]. Briefly, the DDCLC cell can be pumped by a single incident pulses beam with adjustable energy (from a Q-switched Nd:YAG SHG pulse laser, wavelength = 532nm, pulse duration = 8ns, repetition rate = 10Hz, pulse energy = E) at an incident angle of around 10° relative to the cell normal (\mathbf{N}), and the generated lasing signals behind the cell (at a distance of $\sim 2\text{cm}$ from the pumped spot on the cell) for nine randomly chosen oblique angles ($\theta = 0^\circ, 17^\circ, 29^\circ, 35^\circ, 39^\circ, 46^\circ, 57^\circ, 65^\circ,$ and 70°) from \mathbf{N} are measured. To analyze the measured lasing signals from each cell at a specific θ , the reflection spectrum (in the visible region) of that cell, which indicates the CLC band structure, is measured at the same oblique angle. Both the lasing spectrum and the reflection spectrum of each cell are obtained using a fiber-based spectrometer system (USB2000-UV-VIS, Ocean Optics).

3. Results and discussion

Figure 1 presents both the absorption and fluorescence emission spectra (blue and red curves, respectively) of the DDCLC cell (cell 1) in the isotropic phase. The peaks of the absorption and fluorescence spectra of the cell are at about 530 and 566nm, respectively. When the wavelength exceeds 575 (680) nm, the absorption (the fluorescence emission) almost vanishes and can be neglected. Since the wavelength of the pumped pulses is close to 530nm, the laser dyes in each cell can be efficiently excited.

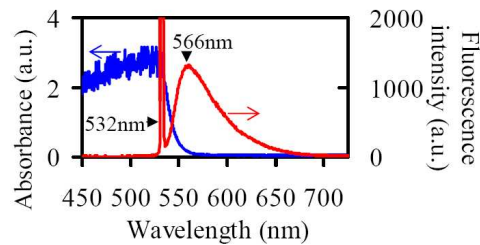


Fig. 1. Measured absorption and fluorescence emission spectra (blue and red curves, respectively) of DDCLC cell (cell 1) in isotropic phase.

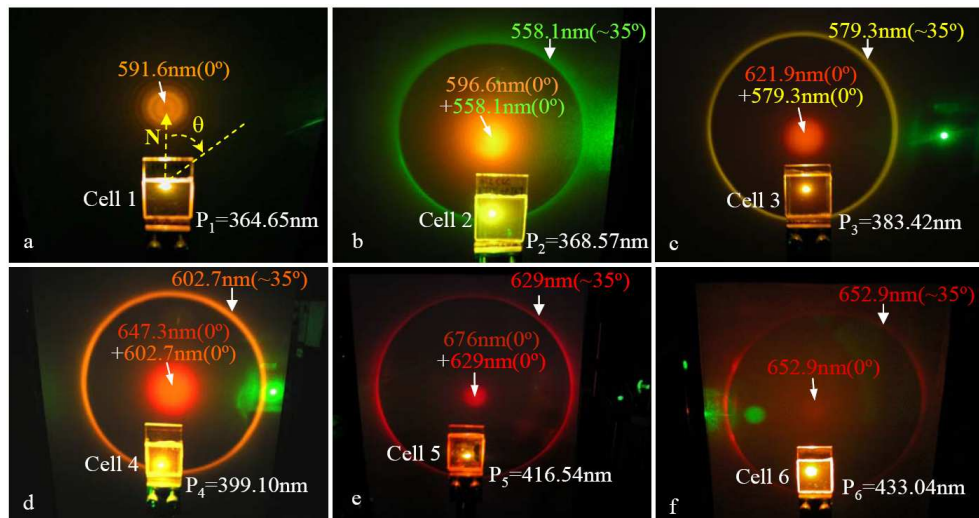


Fig. 2. (a)-(f) Obtained six CCLE patterns when cells 1-6 with pitches P_1 - P_6 , respectively, are excited by the incident pulses with a given pumped energy $E = 10\mu\text{J}/\text{pulse}$, where those $\lambda(\theta)$ marked on these photographs represent the measured wavelengths of the bright lasing signals at the LWE and the SWE measured at 0° (normal lasing emissions) and at the LWE measured at nearly 35° (lasing rings).

Figures 2(a)-2(f) show photographs of six obtained CCLE patterns on the screen (behind each cell) after cells 1-6 are individually excited by incident pumped pulses with the same energy of $E = 10\mu\text{J}/\text{pulse}$. Since each CCLE is distributed conically and symmetrically about \mathbf{N} , the features of the lasing signals emitted in the plane of incidence at various oblique angles, θ , from \mathbf{N} (Fig. 2(a)) can alone be measured and studied without loss of generality. Even if only the lasing signals in the \mathbf{N} direction ($\theta = 0^\circ$, normal lasing emissions) and at nearly 35° (lasing rings) are sufficiently bright to be seen by the naked eye, the lasing signals at other angles can easily be detected using a sensitive spectrometer. Figures 3(a.1)-3(f.1) display the lasing spectra of the six obtained CCLE patterns and the corresponding reflection spectra measured at nine randomly selected oblique angles ($\theta = 0, 17, 29, 35, 39, 46, 57, 65$, and 70°) based on cells 1-6, respectively. Evidently, a lasing peak at any angle in any obtained CCLE that is based on cells 1-6 always occurs close to the LWE and SWE of the CLCRB. Figures 3(a.2)-3(f.2) (3(a.3)-3(f.3)) plot variations in the intensity of the lasing signal at the LWE (SWE) measured at $0-70^\circ$ for cells 1-6, respectively, with the pumped energy. Based on the experimental results in Figs. 3(a.2)-3(f.2) and 3(a.3)-3(f.3), Figs. 4(a)-4(f) plot the variations of the wavelength of the lasing signal at the LWE/SWE ($\lambda_{\text{las}}(\text{LWE})/\lambda_{\text{las}}(\text{SWE})$), represented as \bullet/\blacksquare with the oblique angle, based on cells 1-6, respectively. Consistent with the same simulation steps in our earlier study [42], the simulation results for dispersion relations obtained using Berreman's 4×4 matrix method [43] for planar CLC structures with various pitches of $P_1(364.65\text{nm})$ - $P_6(433.04\text{nm})$ can yield the simulation relations between the wavelengths at the LWE/SWE of the CLC stop band in which $v_g \rightarrow 0$ and $\text{DOS} \rightarrow \infty$ ($\lambda_{\text{LWE}}(v_g \rightarrow 0, \text{DOS} \rightarrow \infty)/\lambda_{\text{SWE}}(v_g \rightarrow 0, \text{DOS} \rightarrow \infty)$), represented as \circ/\square . Figures 4(a)-4(f) plots these simulated results. Notably, Fig. 4 indicates strong consistency between the experimental and simulated results for multi-cells with various pitches. These results verify that these CCLEs are based on photonic band-edge lasing theory for a distributed feedback resonator, as addressed in the authors' previous work [42]. Apparently, Figs. 2-4 indicate that the lasing band of the CCLE at the LWE can be tuned from the short- to the long-wavelength region as the cell pitch is increased from P_1 to P_6 . This particular band-tunability of CCLE due to multiple Bragg modes irradiated at angles other than 0° was observed experimentally for the first time [5,12-14,16-20,24,27,33,37,39].

Based on the experimental results in Figs. 3(a.2)-3(f.2) and 3(a.3)-3(f.3), Figs. 5(a) and 5(b) plot variations in the energy threshold with the cell pitch for lasing emissions measured at different oblique angles at the LWE and SWE, respectively. Several unique features of CCLEs based on cells 1-6, revealed by the experimental results in Figs. 3-5, are discussed below. First, the angular range and the band of the lasing emission in the CCLEs are pitch-dependent. In Figs. 4(a)-4(e), this angular range (band) of lasing emission at the LWE increases from 0 to 17° (591.56 - 581.02nm) to 0 - 46° (676.04 - 601.38nm) as the pitch increases from $P_1 = 364.65\text{nm}$ to $P_5 = 416.54\text{nm}$. These experimental results follow from the fact that, as the pitch increases, the CLCRB and the LWE are both increasingly red-shifted and removed from the absorption band ($\leq 575\text{nm}$) (Figs. 3(a.1)-3(e.1)), causing the fluorescence to propagate within an increased angular range with no re-absorption by the laser dyes, increasing the lasing band. Second, as displayed in Figs. 3(a.1)-3(e.1), the SWE is much closer to the absorption band than the LWE, and so the re-absorption of the fluorescence at the SWE is much stronger than at the LWE. Consequently, the CCLE effect at the SWE is much weaker than that at the LWE, as revealed by the experimental results in Figs. 3(a.2)-3(e.2) and 3(a.3)-3(e.3) and Fig. 5. Third, except for the curve of 0° in Fig. 5(a), all curves in Fig. 5 (including that for 0° in Fig. 5(b)) are concave upward. This experimental results imply that two main factors, absorption and fluorescence intensity, competitively influence the features of the CCLE. Based on a comparison of the experimental results in Figs. 1 and 3(a.1)-3(f.1), when the pitch becomes shorter such that the band edges increasingly overlap the absorption band, or, when the pitch becomes longer and more of the band edges are removed from the absorption band and their fluorescence intensity is decreased, the energy threshold increases as a consequent. The curve for 0° in Fig. 5(a) is an exception because the wavelength of the LWE at 0° for each cell never overlaps the absorption band (Figs. 3(a.1)-3(f.1)). Therefore, as

the pitch increases, the decrease in the fluorescence intensity monotonically increases the energy threshold. Fourth, the three simultaneously obtained lasing signals at the LWE and SWE measured at 0° and at the LWE measured at nearly 35° , displayed in Figs. 2(b)-2(e) and 3(b.1)-3(e.1), are much stronger than those emitted at other oblique angles. The former two (normal lasing emissions) have been commonly observed in studies of DDCLC lasers [2–41]. However, the last one (lasing ring) is identified herein for the first time for DDCLCs. These particularly strong lasing rings (green, yellow, orange and red) at nearly 35° (presented in

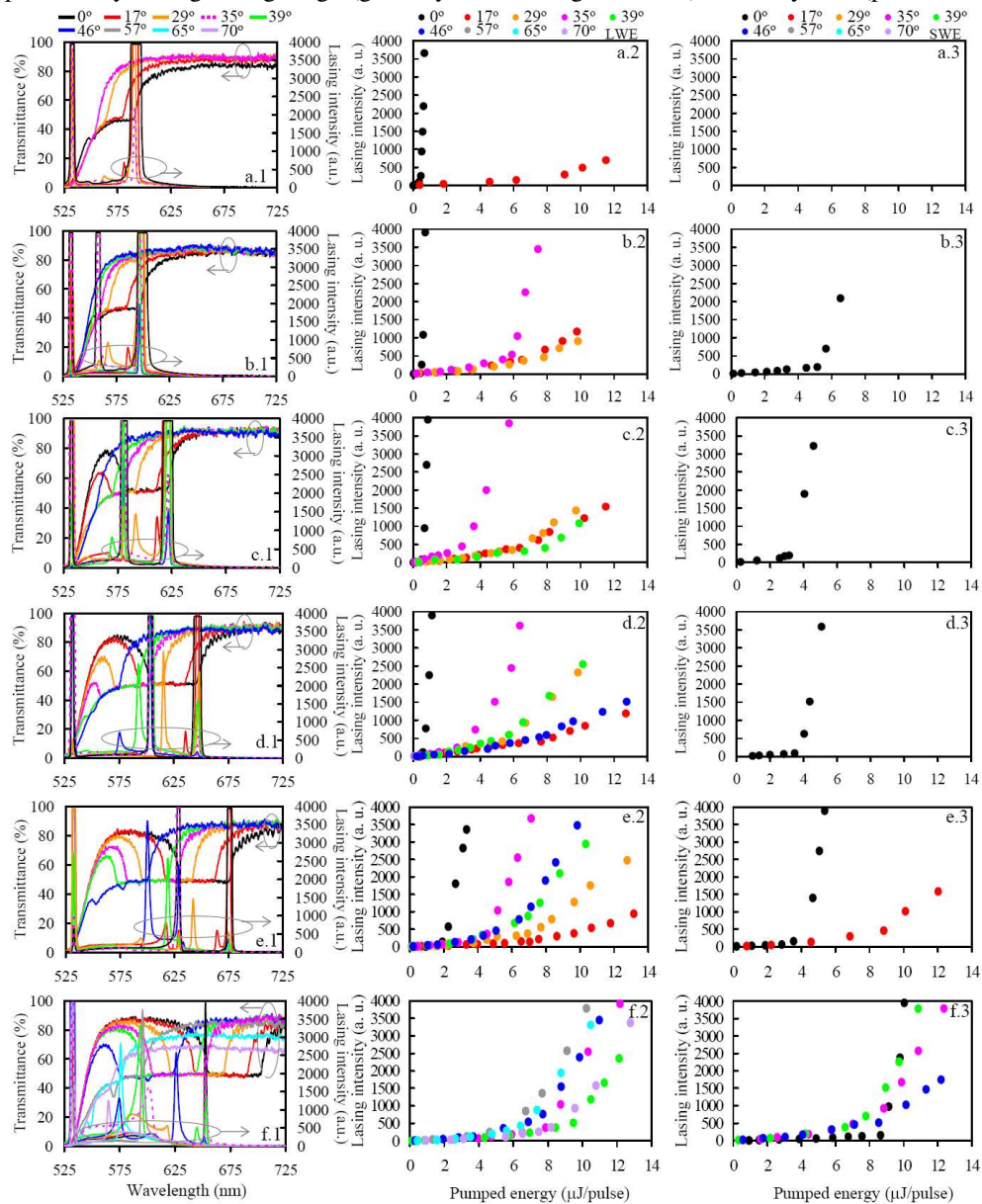


Fig. 3. (a.1)-(f.1) Lasing spectra from CCEs obtained after cells 1-6 are individually excited by incident pulses with $E = 10\mu\text{J/pulse}$ and reflection spectra of cells 1-6, respectively, for oblique angles $\theta = 0-70^\circ$. (a.2)-(f.2) ((a.3)-(f.3)) Variations of intensity of lasing signal in CCEs measured at $\theta = 0-70^\circ$ at the LWE (SWE) with pumped energy based on cells 1-6, respectively.

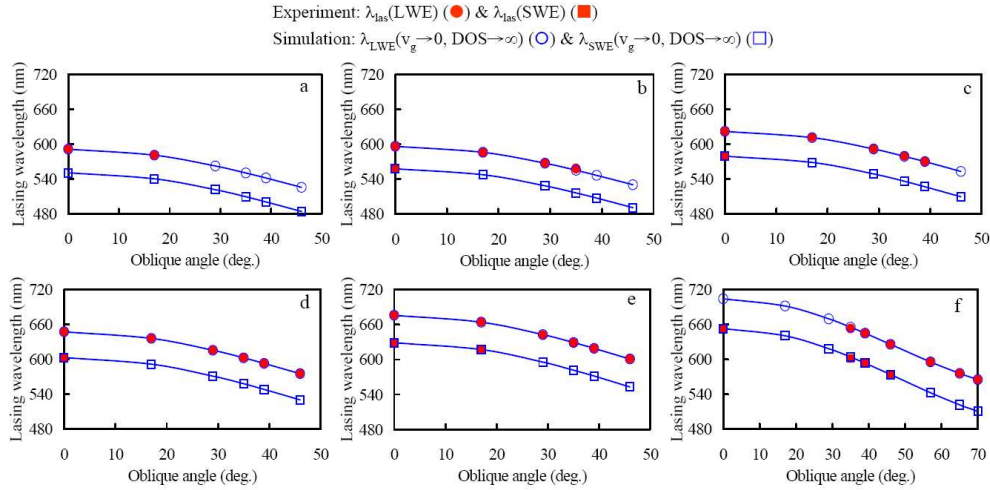


Fig. 4. ● (■) and ○ (□) symbols represent lasing wavelengths measured at the LWE (SWE) of CLC reflection band ($\lambda_{\text{las}}(\text{LWE})$ ($\lambda_{\text{las}}(\text{SWE})$) in Fig. 3) in the experiment and simulated wavelengths at the LWE (SWE) of the CLC stop band in which $v_g \rightarrow 0$ and $\text{DOS} \rightarrow \infty$ ($\lambda_{\text{LWE}}(v_g \rightarrow 0, \text{DOS} \rightarrow \infty)$ ($\lambda_{\text{SWE}}(v_g \rightarrow 0, \text{DOS} \rightarrow \infty)$)), respectively, at oblique angles 0° - 70° .

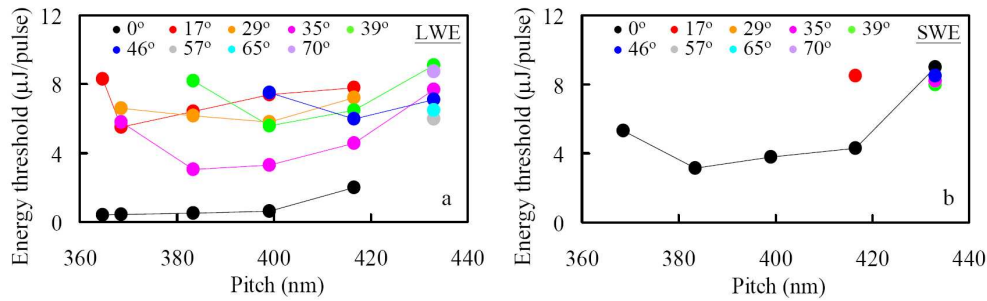


Fig. 5. Variations of energy threshold of lasing signal at the (a) LWE and (b) SWE with pumped energy at various oblique angles from 0° to 70° .

Figs. 2(b)-2(e), respectively) in cells 2-5 have in common that the wavelength of each at 35° is close to the value at which the LWE, measured at an oblique angle of roughly 35° , overlaps the SWE, measured at 0° . Briefly, $\lambda_{\text{LWE}}(35^\circ) = \lambda_{\text{SWE}}(0^\circ)$ (as evident in the reflection spectra measured at 0° and 35° (black and pink, respectively) in Figs. 3(b.1)-3(e.1)). We suggest that beams of fluorescence with the same wavelength ($\lambda_{\text{LWE}}(35^\circ) = \lambda_{\text{SWE}}(0^\circ)$) propagating at nearly 35° and 0° may indirectly reinforce each other because of the enhancements of the associated respective rates of spontaneous emission. This effect may be the main reason why the lasing with $\lambda_{\text{LWE}}(35^\circ)$ is much stronger than those at other nonzero oblique angles, even if spontaneously emitted fluorescence with this wavelength is far from the maximum (at 566nm) of each fluorescence spectrum (Figs. 3(c.1)-3(e.1)). This work does not focus on this effect, but a forthcoming manuscript will systematically address it. Fifth, Figs. 3(f.1)-3(f.3), based on cell 6, reveal a very different CCLE from those based on cells 1-5, associated with which the lasing signal at the LWE of 0° is zero and the lasing signals at the LWE of 35° and at the SWE of 0° both decay substantially, because the fluorescence intensity within the CLCRB of 0° based on cell 6 with a longest P_6 is either zero or very weak. Rather, more lasing signals are generated at the LWEs (SWEs) at the large angles of 46° - 70° (35° - 46°). Not only are the spontaneously emitted fluorescence intensities at the edges of these large angles all strong, but also the simultaneous collapse of the three lasing signals at $\lambda_{\text{LWE}}(0^\circ)$, $\lambda_{\text{LWE}}(35^\circ)$ and $\lambda_{\text{SWE}}(0^\circ)$

similarly promotes the enhancement of the emission rate of the fluorescence that propagates at other angles, yielding such experimental results as found in Figs. 3(f.1)-3(f.3).

This study fabricates for the first time a spatially band-tunable color cone laser that is based on a single DDCLC cell with a pitch gradient along the cell surface which is formed by the successive injection of the above six DDCLC mixtures into the empty cell. Figure 6(a) presents the formed cell as well as the reflection pattern of one incident white beam from the cell with a continuous distribution of green to red wavelengths from the left to the right of the pattern. When the incident pulses excite the left to the right position of the cell, a spatially-band tunable CCLE distributed from short- to long-wavelength region can be obtained, as revealed by the patterns from the left to the right, photographed in Fig. 6(b) (which are similar to the CCLE patterns in Figs. 2(a)-2(f)), in which the green background is produced by the scattering of the incident pumped pulses of light.

Experimental results in a forthcoming manuscript will show that the performance characteristics (e.g., the energy threshold and slope efficiency) of the CCLE are significantly dependent on the degree of perfection of the CLC structure. The use of imperfect cells is one of the possible reasons for why other authors did not observe such a wide-angle lasing for Bragg modes.

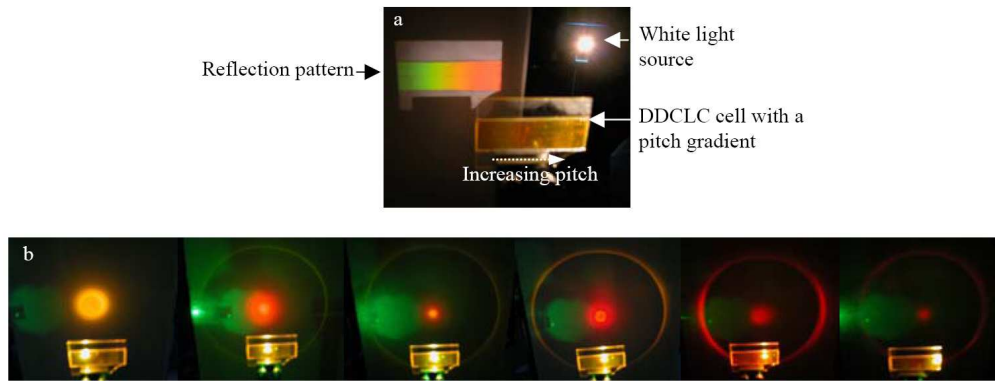


Fig. 6. (a) Reflection pattern from DDCLC with a pitch gradient obtained under illumination by one white light source. (b) Spatially-tunable CCLE pattern (from left to right) obtained by excitation by incident pulses with $E = 10\mu\text{J/pulse}$ from the left to the right of the gradient-pitched DDCLC.

4. Conclusion

This study demonstrates for the first time a novel band-tunable color cone lasing emission (CCLE) based on dye-doped cholesteric liquid crystal (DDCLC) films with different pitches. Experimental results show that the lasing band of the formed CCLE can be tuned from short- to long-wavelength region, measured within different ranges of oblique angle, with decreasing the chiral concentration and thus increasing the pitch of the CLC. Some unique lasing features of the formed CCLE are also identified and explained. Moreover, a spatially band-tunable color cone laser, based on a DDCLC cell with a gradient pitch, is developed as a real application.

Acknowledgments

The authors would like to thank the National Science Council of the Republic of China, Taiwan (Contract No. NSC 97-2112-M-006-013-MY3) and the Advanced Optoelectronic Technology Center, National Cheng Kung University, under projects from the Ministry of Education for financially supporting this research. Ted Kroy is appreciated for his editorial assistance.